ACTA IMEKO
ISSN: 2221-870X
December 2017, Volume 6, Number 4, 75-79

Performing accelerometer calibration using homodyne laser interferometry with displacements smaller than $\lambda/4$

Christiaan S. Veldman

National Metrology Institute of South Africa, CSIR Campus, Pretoria, South Africa

ABSTRACT
Laser interferometry is a preferred method of realizing the National Measurement Standard for vibration by National Metrology Institutes. Laser interferometry is well documented and its detailed implementation described in ISO 16063, part 11. When employing Homodyne demodulation of the quadrature signals, the minimum peak to peak displacement is limited at $\lambda/4$, or half a circle when viewed on a Lissajous plot. A technique whereby the exciter armature is continuously displaced (continuously varying reference) is described. The reference position is varied by adding a DC-ramp signal and the resulting unwanted slope is removed using high pass filtering. This technique enables one to extend the vibration calibration frequency range from 10 kHz up to 20 kHz with an applied acceleration of 200 m/s².

Section: RESEARCH PAPER

Keywords: primary; accelerometer; calibration; homodyne; laser interferometry

Citation: Christiaan S. Veldman, Performing accelerometer calibration using homodyne laser interferometry with displacements smaller than λ/4, Acta IMEKO, vol. 6, no. 4, article 12, December 2017, identifier: IMEKO-ACTA-06 (2017)-04-12

Editor: Paul Regtien, Measurement Science Consultancy, The Netherlands

Received June 29, 2017; **In final form** November 30, 2017; **Published** December 2017

Funding: This work was supported by the Department of Trade and Industry, South Africa

Corresponding author: Ian Veldman, e-mail: CSVeldman@NMISA.org

1. INTRODUCTION

National Metrology Institutes (NMIs), as the custodian of their country's National Measurement Standards (NMS), achieve the highest possible accuracy for measurement units through primary measurement techniques. By doing so, the NMI shortens the traceability chain, resulting in the realisation of the smallest Uncertainty of Measurement (UoM). In Vibration Metrology, the unit for acceleration [1] is realised using laser interferometer systems. This provides "direct" traceability to the Système International d'Unités (SI) unit for Length, the metre (m) and Time, the second (s).

The growth and extension in the application of vibration measurements by industry encourages sensor manufacturers to develop accelerometers that will meet the requirements of these new applications. In many instances, the need is not for higher accuracy devices, but devices that extend the dynamic measurement range, for level- as well as the frequency range. The extension of the frequency range provides new calibration challenges for NMIs.

Accurate earth quake monitoring and design improvements relating to seismic activities are some examples driving the demand for extended low frequency measurement ranges. The accelerometer output (sensitivity) is generally the limiting factor for extending the calibration frequency range lower. This is due to reduced acceleration levels that can be generated as the vibration frequency decreases, and the displacement is kept constant. In this instance, the maximum peak to peak displacement limit of the vibration exciter becomes the limiting factor.

On the other end of the frequency spectrum, the demand for accurate acceleration measurements above 10 kHz are driven by developments in predictive maintenance programs, modal analysis and shock measurement, to name but a few. Here, the challenge for accurate calibration by laser interferometry are set by the minimum displacement that can be accurately measured using the currently implemented homodyne interferometry methods. The peak displacement limit being $\lambda/4$ or about 160 nm for a red Helium-Neon (HeNe) laser.

In Section 2, the application of laser interferometry as

described in the relevant ISO standards is briefly discussed, highlighting the peak displacement requirement as a limiting factor covered in this publication. The author considers some of the current methods available in literature. The author proposes a modification to method 3 of [2] in Section 3. This then proposes a method that enables the use of homodyne demodulation for displacements < $\lambda/4$. A comparison of results supporting the accuracy of this method is made in Section 4 with the conclusions drawn reported in Section 5.

2. ACCELEROMETER CALIBRATION USING LASER INTERFEROMETRY

Standardized approaches for the calibration of accelerometers by primary means are described in ISO 16063-11 [2]. For the calibration of any vibration transducer, metrological traceablility to the International System of Units (SI), the three basic parameters to be determined are:

- time, obtained from the generated sinusoidal vibration period
- transducer output, generally a voltage measurement
- vibration amplitude, obtained by laser interferometry (as in this context).

In this ISO standard [2], three different methods of calibration by laser interferometry are described;

- Method 1: Ratio Counting Method (RCM)
- Method 2: Minimum Point Method (MPM)
- Method 3: Sine Approximation Method (SAM)

Of interest for this paper is Method 3: Sine Approximation Method.

At the heart of Method 3 is the homodyne laser interferometer system with two optical paths in quadrature as depicted in Figure 1. The transducer output- and time determination aspects are not considered in this article as they have no direct influence in the topic of discussion and have been dealt with extensively in [2]-[4], [7].

The interference signals produced by the interferometer are converted into electrical signals, resulting in the In-phase (I) and Quadrature (Q) signals (I-Q data) of interest. After appropriate signal conditioning, including quadrature correction if required, the I-Q data is demodulated using the arc-tangent function with appropriate phase unwrapping. This is done to obtain the complex (magnitude and initial phase) of the peak to peak displacement of the generated vibration signal. Finally, the displacement is differentiated twice to obtain the peak acceleration.

Plotting the I-Q data on the x- and y axis of a Cartesian coordinate system results in a Lissajous figure, shown in Figure 2. For ideal I-Q data, the Lissajous figure will form a perfect circle. Unfortunately, actual measurement data always contain imperfections in terms of dc-offsets, differences in gain between the I & Q data channels and the I-Q data not being 100 % in quadrature, to name a few of the more pertinent error sources. These result in errors in the final calculated magnitude and initial phase of the vibration signal.

For vibration amplitudes ≥ $\lambda/2$, a full (complete) circle is formed. With sufficient data points to describe a circle, data fitting algorithms [5], [6] can be applied to measurement data to correct for imperfections.

The accuracy of these algorithms is dependent on the amount of data (number of data points), the fraction of the geometry represented by the data available, ideally ≥ π radians, and other factors as reported in [7]. Data covering a full circle is available for peak to peak displacement of ≥ $\lambda/2$.

In instances where the vibration amplitudes < $\lambda/2$, the data describes only part of a circle. As the vibration amplitude reduces further, even less information describing the circle is available. A critical point is reached when the vibration amplitude is < $\lambda/4$, in which case the available data describes less than half a circle as shown in Figure 2.

This limited data (knowledge) of the circle results in a poorly representative circle. This results in the fitting (data correction) algorithm producing results which may not be sufficiently valid [7]. To ensure the high accuracy required for displacement measurement using laser interferometry, the metrologist has three options:

1. Increase the vibration level to ≥ $\lambda/4$.
2. Develop a more robust data correction algorithm.
3. Produce the section(s) of the circle that is needed to complete the circle.

Option 1 is impractical and generally impossible, due to the physical limitation of the vibration exciter at high frequencies. Option 2 could for instance be achieved using fitting methods as described in [8].

Bruns et al [9] reported on the implementation of a dual frequency method to be used for high frequency calibration of velocity transducers. The method reported by him achieves the requirements for Option 3. The signal processing for the method described in [9] requires the following data fit to be solved:

$$v(t) = a_1 \cdot \sin(\omega_1 t) + b_1 \cdot \cos(\omega_1 t) + a_2 \cdot \sin(\omega_2 t) + b_2 \cdot \cos(\omega_2 t) + c \quad (1)$$

As can be seen above (1) contains more unknowns to be solved, thus requiring more processing time and computing

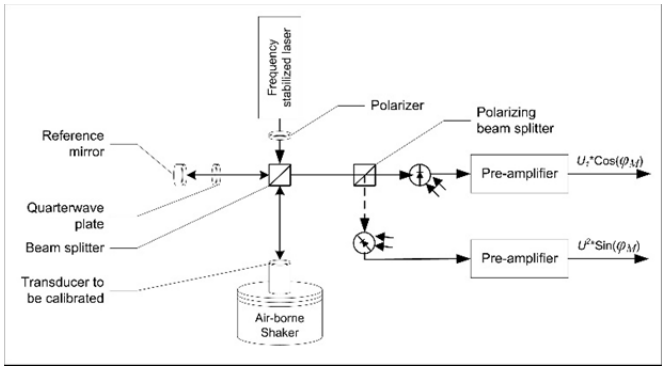

Figure 1. Schematic diagram of a quadrature laser interferometer calibration setup.

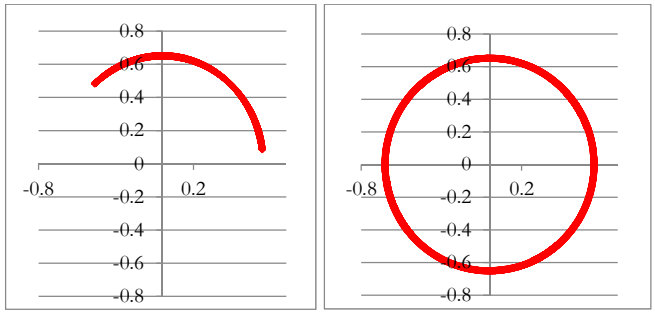

Figure 2. On the left, a Lissajous figure of a 10 kHz vibration signal with a displacement < $\lambda/4$. On the right, a Lissajous figure of a 10 kHz vibration signal with a displacement < $\lambda/4$ added to a dc-ramp signal. The axis units are arbitrary.

power and computer memory.

The author is proposing the implementation of a novel system adaptation of trending laser interferometer calibration systems to achieve Option 3. The proposed implementation requires very little, if any, additional hardware and requires only minor adjustments to the measurement procedure and software procedure as reported in Section 3.

3. VARYING POSITION CALIBRATION

3.1. Implementation concept

The proposed system design solution is based on the approach in realising the circle in sections and then "stitching" these segments of the circle together to form a full circle. In doing so, gathering all the information required to describe the circle with sufficient accuracy.

Consider an instance where the vibration amplitude equals $\lambda/16$ (± 20 nm for a red HeNe laser). This will result in the data points describing only an eighth of a circle (⅛◙). Under ideal circumstances (absence of drift and other influences) and with perfect equipment, the displayed ⅛◙ will be stationary in its position on the oscilloscope. Should one lift the exciter by $\lambda/16$, the ⅛◙ will rotate by 45° around the centre point of the circle. The direction of this rotation is irrelevant. By continuing this process of lifting the exciter by $\lambda/16$, the rotating ⅛◙ will eventually have moved through 360° and completed the circle.

With electrodynamic exciters, capable of 8 mm peak to peak displacements, repositioning the exciter armature by $\lambda/16$ is more practical and can easily be achieved. The change in position of the armature (not considering the desired vibration being generated) is easily accomplished by applying a dc voltage offset to the vibration signal. This will facilitate the repositioning of the armature surface.

Rather than repositioning the armature in $\lambda/16$ steps, a continuous relocation of the armature surface is accomplished by adding a ramped dc voltage offset to the vibration signal. This introduces a continues rotation of the circle fragment produced by the applied high frequency vibration signal. The applied dc offset signal must introduce a displacement (movement) of the armature top surface of at least $\lambda/4$. This offset the armature position should continue for the full time duration of the vibration signal is being measured. The resulting effect of completing the circle through varying the position of the armature and capturing the sampled data in various locations of the Lissajous figure is depicted in Figure 3. Figure 3 shows segments of the circle captured during the vibration measurement time. Each segment is presented in a different colour.

3.2. System configuration & implementation

The minimum calibration system components required to perform accelerometer calibration using homodyne demodulation typically consist of:

1. a laser interferometer with quadrature outputs
2. a vibration exciter
3. a power amplifier (ac input)
4. a signal generator (single channel)
5. a transducer output signal conditioning unit
6. a three-channel data acquisition unit

In comparison with this, the proposed varying position calibration system would consist of:

1. a laser interferometer with quadrature outputs
2. a vibration exciter

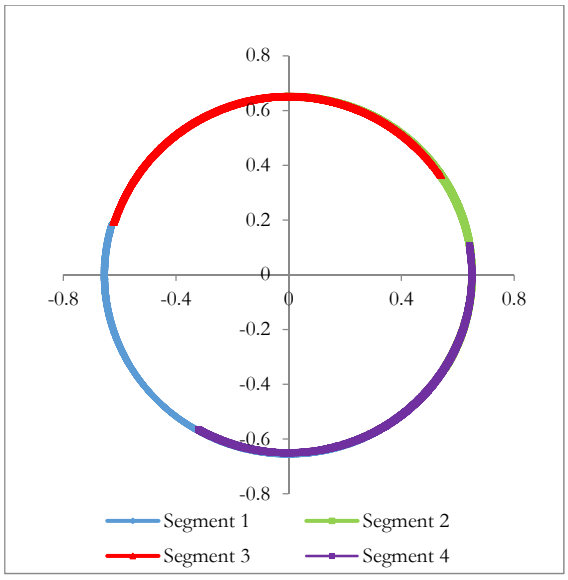

Figure 3. Segments of four Lissajous figures completing a full circle.

3. a dual input power amplifier (dc- and ac inputs)
4. a dual channel signal generator
5. a transducer output signal conditioning unit
6. a three-channel data acquisition unit
7. an attenuator (optional)

A schematic diagram of such a system configuration is shown in Figure 4. The continuous movement of the armature reference surface, that is the surface on which the laser is focused, is achieved by adding the dc offset signal by means of a ramp signal, or a saw tooth signal to the required vibration signal. This can be achieved via the power amplifier's dc signal input or employing a circuit that can add the two signals together.

An important point to be considered is that the amplitude of the dc offset shall be chosen such that exciter displacement specification is not exceeded. A practical starting point could be a 0.5 mm peak to peak displacement. This setting can be accomplished experimentally. With the power amplifier gain set to the required level for the sinusoidal vibration, add the dc-ramp signal to the DC input of the power amplifier. Increase the amplitude of the ramp signal until the desired peak to peak displacement is obtained. To achieve this in the setup (combination of generator, power amplifier and electrodynamic

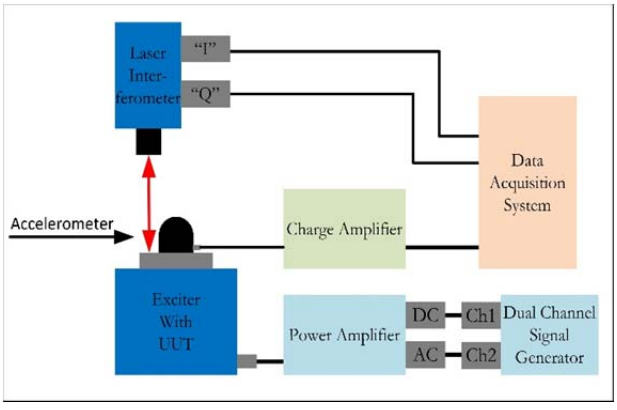

Figure 4. System diagram for a varying position calibration system.

exciter) used by the author, an attenuator had to be inserted between Channel 2 of the generator (used for generating the dc ramp signal) and the dc input of the power amplifier. This was required as the generator used could not generate a dc-ramp signal with a small enough amplitude.

To ensure data capturing is executed on the ramp portion of the signal (and not while the ramp signal is transitioning back to "zero"), one could use the ramp signal as a trigger input to the data acquisition system. Another practical approach is to set the period of the dc-offset signal to the total time required to sample the number of vibration periods of interest. For instance, when sampling 1 000 periods of a 10 kHz vibration signal, select a dc-ramp period of > 0.1 s.

3.3. Signal processing

The dc offset ramp signal will be present in the acceleration time signal as it contains the acceleration signal super-imposed onto the dc offset ramp signal as shown in Figure 5. This slope (trend) present in the data will negatively influence the peak value determination of the vibration signal. This unwanted component in the acceleration signal can easily be removed by applying a high pass filter to remove the dc-component. For the removal of the dc component, the author implemented a high pass filter with a cut-off frequency of 1.2 Hz. This cut-off frequency is sufficiently high to remove the dc, yet well below the vibration frequency of interest. The filtering is adequate if the slope is completely removed. Other requirements for this high pass filter are the same as for the all other filtering applied during the calibration procedure. Of special note is the requirement to ensure a linear phase response filtering the data, when phase of the sensitivity is to be determined as well.

The removal of the ramp (trend) from the acceleration time series is required for accurate sine-fitting results. The post high pass filtered vibration signal is shown in Figure 6.

The implementation of this calibration method does not require any additional or special signal processing as far as the arctangent demodulation, phase unwrapping and sine approximation using (2) to determine the magnitude and initial phase of the acceleration signal is concerned.

$$\varphi_{Mod}(t) = A \cdot \cos(\omega t) - B \cdot \sin(\omega t) + C \qquad (2)$$

where

$A = \hat{\varphi}_M \cos\theta_s$

$B = \hat{\varphi}_M \sin\theta_s$

C is a constant

ω is the vibration radian frequency, $\omega = 2\pi f$

θ_s is the initial phase angle of the displacement

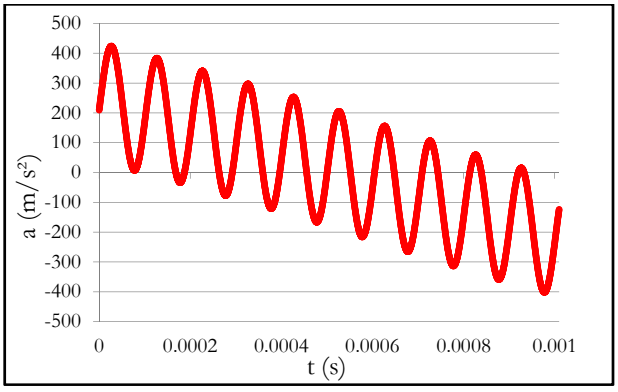

Figure 5. 10 kHz vibration signal with dc-ramp present.

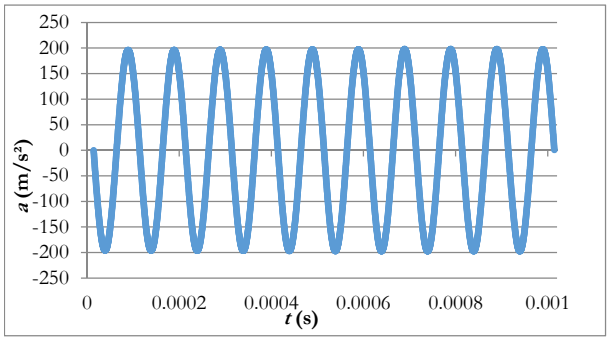

Figure 6. 10 kHz vibration signal with dc-ramp effect removed using high-pass filtering.

4. PERFORMANCE EVALUATION

The proposed calibration technique was validated through the calibration of a single ended laboratory standard accelerometer. The device used was an ENDEVCO 2270M8 accelerometer with a nominal sensitivity of 0.22 pC/(m/s²). The sensing element of this accelerometer is made of P-10 crystal material and it has a resonant frequency of 55 kHz.

NMISA [10] has calibration history data for this device dating back to 2001. Until recently, calibrations for this device were performed up to 10 kHz only. In 2004, NMISA had the device calibrated by the PTB [11]. The calibration by PTB covered the frequency range 10 Hz to 20 kHz.

The accelerometer's calibrated sensitivities reported by NMISA in January 2017 [12] using the proposed varying position method were compared with the calibrated sensitivities reported by PTB [11] in 2004. The sensitivities were evaluated by calculating the Normalised Error (En)values for each frequency point using

$$E\text{n} = \frac{S_{\text{NMISA}} - S_{\text{PTB}}}{\sqrt{U_{\text{NMISA}}^2 + U_{\text{PTB}}^2}} \qquad (3)$$

where

S_{NMISA} is the charge sensitivity reported by NMISA

U_{NMISA} is the expanded uncertainty of measurement reported by NMISA

S_{PTB} is the charge sensitivity reported by PTB

U_{PTB} is the expanded uncertainty of measurement reported by PTB

The calculated En values were used as an indication of how well the reported sensitivities compared within the stated uncertainty of measurement.

The calibrated sensitivity values, associated uncertainty of measurement and calculated En values are reported in Table 1 and shown in graphical format in Figure 7. Only sensitivities at key frequency points for frequencies below 10 kHz are reported. The results for frequencies above 10 kHz being reported in more detail, that is for more frequencies. It can be seen from the Table 1 that all the reported En values are $< |1|$, indicating there is good agreement between the sensitivity values reported by PTB and the sensitivity values measured by NMISA using this method.

5. CONCLUSIONS

In this publication, the author reported on the successful implementation of a novel technique to extend the implementation of homodyne laser interferometry as described

Table 1. Calculated E_n values for NMISA vs PTB sensitivity calibrations.

Frequency	PTB		NMISA		E_n
(Hz)	S_{qa} (pC/(m/s^2))	U_c (%)	S_{qa} (pC/(m/s^2))	U_c (%)	
80	0.2017	0.2	0.2019	0.3	0.30
160	0.2018	0.2	0.2018	0.3	0.03
1 000	0.2018	0.2	0.2020	0.3	0.31
5 000	0.2041	0.5	0.2040	0.5	0.08
10 000	0.2117	0.5	0.2107	1.2	0.37
10 500	0.2126	1.0	0.2115	1.2	0.33
11 000	0.2135	1.0	0.2125	1.2	0.29
12 000	0.2175	1.0	0.2154	1.2	0.61
12 500	0.2183	1.0	0.2164	1.5	0.49
13 000	0.2198	1.0	0.2177	1.5	0.52
13 500	0.2206	1.0	0.2191	1.5	0.39
14 000	0.2206	1.0	0.2195	1.5	0.28
14 500	0.2224	1.0	0.2204	1.5	0.49
15 000	0.2245	1.0	0.2221	1.5	0.60
15 500	0.2262	1.5	0.2241	2.0	0.37
16 000	0.2281	1.5	0.2258	2.0	0.40
16 500	0.2299	1.5	0.2275	2.0	0.42
17 000	0.2317	1.5	0.2294	2.0	0.39
17 500	0.2339	1.5	0.2310	2.0	0.50
18 000	0.2358	1.5	0.2329	2.0	0.49
18 500	0.2376	1.5	0.2352	2.0	0.41
19 000	0.2405	1.5	0.2357	2.0	0.82
19 500	0.2425	1.5	0.2388	2.0	0.62
20 000	0.2448	1.5	0.2412	2.0	0.60

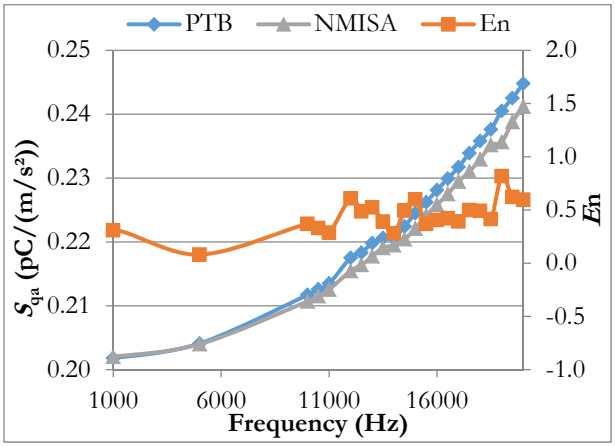

Figure 7. Reported Charge Sensitivity and *En* values.

in ISO 16063 part 11, method 3, below the specified displacement amplitude of $\geq \lambda/4$. This technique, continuous varying position calibration, enables the metrologist to extend the calibration frequency for accelerometer calibration using primary methods beyond 10 kHz and potentially above 20 kHz.

The implementation of this method has the added advantage of reducing the acceleration amplitude required to perform the calibration, placing a smaller demand on the vibration exciter used. Lower acceleration levels require less power, which generate less heat. This also reduces the heating effect on the accelerometer being calibrated.

The method was validated by comparing calibration results using this method with calibration results reported by PTB. The calculated *E*n values were all smaller than one, indicating good correlation between the sensitivities reported by the two NMIs. The resulting *E*n also serve as validation of the UoM estimated by NMISA for this method.

REFERENCES

[1] ISO 16063-1, Methods for the calibration of vibration and shock transducers -- Part 1: Basic concepts.

[2] ISO 16063-11, Methods for the calibration of vibration and shock transducers -- Part 11: Primary vibration calibration by laser interferometry.

[3] Veldman C.S., "A novel implementation of an ISO standard for primary vibration calibration by laser interferometer", Metrologia 40 (2003), pp. 1-8.

[4] von Martens H J, Taubner A, Wabinski W, Link A and Schlaak H-J, Traceability of vibration and shock measurements by laser interferometry", Measurement, 28, (2000), pp. 3–20.

[5] Heydeman P.L.M., Determination and correction of quadrature fringe measurement errors in interferometers. Applied Optics, 20, No. 19, (1981), pp. 3382-3384.

[6] Wu C-M, Su C-S and Peng G-S Correction of nonlinearity in one-frequency optical interferometry, Meas. Sci. Technol. 7, (1996), pp. 520–4.

[7] Sun Q., Wabinski W., Bruns T., Investigation of primary vibration calibration at high frequencies using the homodyne quadrature sine-approximation method: problems and solutions. Meas. Sci. Technol. 17 (2006) 2197–2205.

[8] T. Poˇzar and J. Moˇzina, "Enhanced ellipse fitting in a two-detector homodyne quadrature laser interferometer", Meas. Sci. Technol. 22 (2011).

[9] Bruns T., Blume F., Täubner A., "Laser vibrometer calibration at high frequencies using conventional calibration equipment", XIX IMEKO World Congress, September, (2009), pp. 6−11.

[10] Veldman C.S., "History file: VS-Std-04", NMISA, 2017.

[11] von Martens H. J., "Calibration certificate accelerometer transfer standard", 1.31-894/0704, PTB-097-2004, 2004.

[12] Veldman C.S., "Certificate of calibration of an accelerometer", AV\VS-3465, NMISA, 2017.